Plant Cell Physiol. 45(12): 1749–1758 (2004)

Rapid Paper

Zinc Transporter of *Arabidopsis thaliana* AtMTP1 is Localized to Vacuolar Membranes and Implicated in Zinc Homeostasis

Yoshihiro Kobae [1], Tomohiro Uemura [2], Masa H. Sato [2], Miwa Ohnishi [3], Tetsuro Mimura [3], Tsuyoshi Nakagawa [4] and Masayoshi Maeshima [1, 5]

[1] *Laboratory of Cell Dynamics, Graduate School of Bioagricultural Sciences, Nagoya University, Nagoya, 464-8601 Japan*
[2] *Graduate School of Human and Environmental Studies, Kyoto University, Kyoto, 606-8501 Japan*
[3] *Department of Biology, Faculty of Science, Kobe University, Kobe, 657-8501 Japan*
[4] *Department of Molecular and Functional Genomics, Shimane University, Matsue, 690-8504 Japan*

Cation diffusion facilitator (CDF) proteins belong to a family of heavy metal efflux transporters that might play an essential role in homeostasis and tolerance to metal ions. We investigated the subcellular localization of *Arabidopsis thaliana* AtMTP1, a member of the CDF family, and its physiological role in the tolerance to Zn using MTP1-deficient mutant plants. AtMTP1 was immunochemically detected as a 43 kDa protein in the vacuolar membrane fractioned by sucrose density gradient centrifugation. The expression level of AtMTP1 in suspension-cultured cells was not affected by the Zn concentration in the medium. When AtMTP1 fused with green fluorescent protein was transiently expressed in protoplasts prepared from *Arabidopsis* suspension-cultured cells, green fluorescence was clearly observed in the vacuolar membrane. A T-DNA insertion mutant line for *AtMTP1* displays enhanced sensitivity to high Zn concentrations ranging from 200 to 500 μM, but not to Zn-deficient conditions. Mesophyll cells of the *mtp1-1* mutant plants grown in the presence of 500 μM Zn were degraded, suggesting that Zn at high concentrations causes serious damage to leaves and that AtMTP1 plays a crucial role in preventing this damage in plants. Thus we propose that AtMTP1 is localized in the vacuolar membrane and is involved in sequestration of excess Zn in the cytoplasm into vacuoles to maintain Zn homeostasis.

Keywords: *Arabidopsis* — Cation diffusion facilitator — Metal ion homeostasis — Vacuolar membrane — Zinc transporter.

Abbreviations: AHA3, the third isoform of plasma membrane H^+-ATPase; ER, endoplasmic reticulum; GFP, green fluorescent protein; MTP, metal-tolerant protein; VHA-a, subunit a of vacuolar membrane H^+-ATPase; MES, 2-(*N*-morpholino) ethanesulfonate.

Introduction

Zinc, a micronutrient, is essential for all organisms and plays an important role in key structural motifs in transcriptional regulatory proteins and other enzymes (Marschner 1995). However, Zn can be toxic to the plant at excess concentrations, causing symptoms such as chlorosis. A Zn-hyperaccumulating plant species *Arabidopsis halleri* accumulates a large amount of Zn without developing toxicity symptoms (Dräger et al. 2004). The Zn concentration in leaves is 100-fold higher than that in other species, such as *A. lyrata* and *A. thaliana*. The hyperaccumulation of metals necessitates metal detoxification, for instance by sequestration or chelating of metals ions (Clemens et al. 2002). In *A. halleri*, Zn was accumulated predominantly in the vacuoles of leaf mesophyll cells and a ring-shaped narrow region at the base of trichomes (Küpper et al. 2000). Zn has been proposed to exist predominantly as a complex with malate in leaf mesophyll vacuoles (Zhao et al. 2000, Sarret et al. 2002).

Members of the cation diffusion facilitator (CDF) family including MTP1 (metal tolerance protein, previously ZAT) are thought to transport heavy metals into the vacuoles of leaf epidermal cells in the metal ion-hyperaccumulating plants (hyperaccumulators) (Küpper et al. 1999, Persans et al. 2001, Delhaize et al. 2003). The Zn tolerance of *A. halleri* has been thought to be due to an increased copy number of the MTP1 gene and an enhanced level of transcription (Becker et al. 2004, Dräger et al. 2004).

Zn transport activity of MTP1 in *Arabidopsis thaliana* (AtMTP1) was demonstrated by using reconstituted proteoliposomes of the protein expressed in *Escherichia coli* (Bloß et al. 2002) and by a yeast complementation assay with a Zn-hypersensitive double mutant of ZRC1 and COT1 (*zrc1/cot1*) (Dräger et al. 2004, Kim et al. 2004). AtMTP1 has 92% identity with *A. halleri* AhMTP1-3 (Becker et al. 2004, Dräger et al. 2004). Ectopic expression of AtMTP1 in *A. thaliana* resulted in enhancement of Zn resistance (van der Zaal et al. 1999). The increased tolerance to Zn is thought to be due to

[5] Corresponding author: E-mail: maeshima@agr.nagoya-u.ac.jp; Fax, +81-52-789-4096.

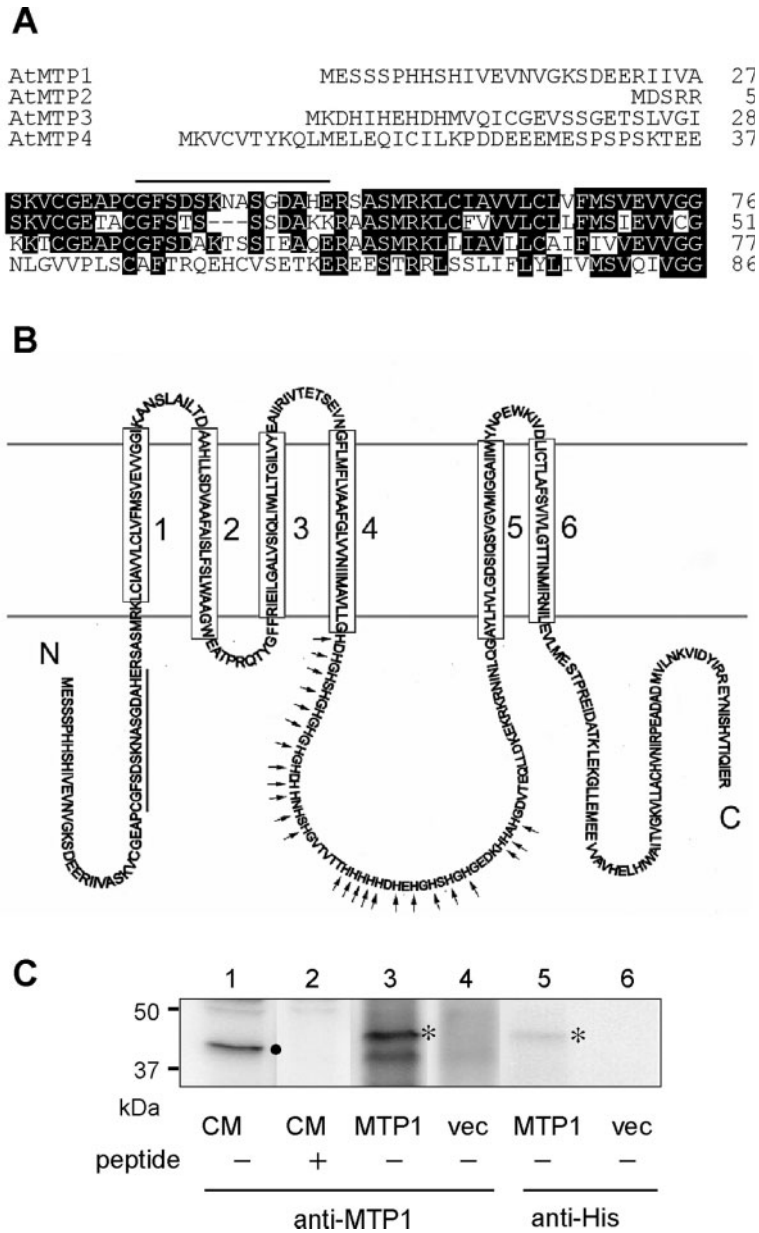

Fig. 1 (A) Alignment of N-terminal amino acid sequences of *A. thaliana* AtMTP1, AtMTP2, AtMTP3 and AtMTP4. The alignment was obtained using ClustalW alignment (Thompson et al. 1994). Identical amino acids are shown in white on a black background. The amino acid sequence used for the antigen peptide is overlined. The residue numbers are shown to the right of each sequence. (B) Hypothetical membrane topology of AtMTP1 predicted by hydropathy analysis. N and C mark the N- and C-termini, respectively. Boxes indicate transmembrane domains and the vertical line indicates the sequence used for antibody preparation. Arrows indicate histidine residues in a His-rich loop. (C) Immunoblot of AtMTP1 protein in membranes. Crude membrane preparations from *A. thaliana* 'Deep' cells (CM, lanes 1 and 2), *S. cerevisiae* expressing AtMTP1 (MTP1, lanes 3 and 5) and *S. cerevisiae* transformed with empty vector (vec, lanes 4 and 6). Immunoblotting was carried out with the polyclonal AtMTP1-specific antibodies (lanes 1–4) and anti-(His tag) antibodies (lanes 5 and 6). For the control experiment, the corresponding authentic peptide was added into the antibody solution prior to the immunostaining. A dot indicates the position of AtMTP1 and the asterisks indicate the position of His-tagged AtMTP1. Molecular mass markers with the size indicated in kDa.

sequestration of Zn into vacuoles through the ectopically expressed AtMTP1. However, neither the subcellular location of AtMTP1 nor the Zn sequestration organelle has been reported.

Interestingly, AtMTP1 protein was annotated to a vacuolar membrane protein prepared from suspension-cultured cells (Shimaoka et al. 2004) grown under standard conditions. In this study, we analyzed the subcellular localization of AtMTP1 using a specific antibody prepared against AtMTP1 and a fusion protein with green fluorescent protein (GFP). We also investigated phenotypic properties of the *A. thaliana AtMTP1*-knockout mutant.

Results

Immunological detection of MTP1 protein

To determine the subcellular localization of AtMTP1 protein, we prepared an anti-peptide antibody against the N-terminal hydrophilic region of AtMTP1. The peptide sequence is characteristic of AtMTP1 compared with three other AtMTPs (Fig. 1A). The membrane topology of AtMTP1 predicted by the hydropathy analysis is shown in Fig. 1B. AtMTP1 shares a common sequence Gly–Phe–Ser–Asp with AtMTP3. However, the antibody against this peptide may not react with AtMTP3, because antibodies strictly recognize amino acid sequences with more than six residues. Furthermore, there was no identi-

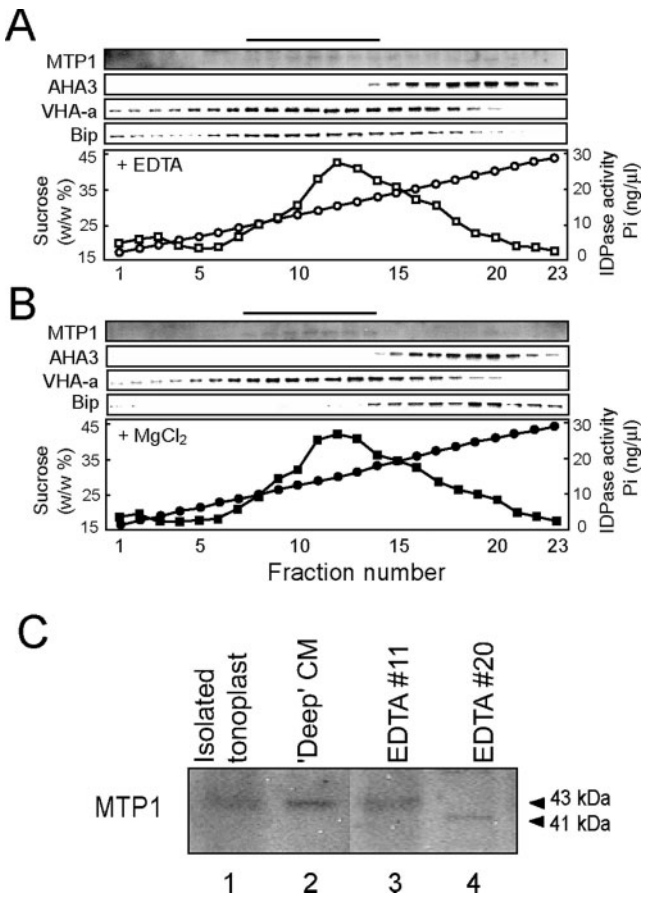

Fig. 2 Subcellular localization of AtMTP1. Microsomal fractions were prepared from *A. thaliana* roots in the presence of 2 mM EDTA (A) or 2 mM $MgCl_2$ (B) and then subjected to sucrose density gradient centrifugation. Proteins in the fractions were electrophoresed, blotted, and immunodetected using antibodies against AtMTP1, plasma membrane H^+-ATPase (AHA3), vacuolar membrane H^+-ATPase subunit a (VHA-a) and BiP (ER marker). The activity of Golgi IDPase was assayed (open and closed squares). The sucrose concentration is shown as open and closed circles. (C) Immunoblot of the isolated vacuolar membrane of *A. thaliana* suspension-cultured cells ('Deep') (lane 1), crude membrane fraction prepared from 'Deep' cells (lane 2), and fractions 11 (lane 3) and 20 (lane 4) after centrifugation of the sample with EDTA. Anti-AtMTP1 antibodies were used. The main band of 43 kDa and a faint band of 41 kDa were marked.

cal peptide sequence in the total proteins of *A. thaliana* in the TAIR Blast 2.0 database (http://www.arabidopsis.org/Blast/).

As shown in Fig. 1C, a 43 kDa protein was detected in an immunoblot with the anti-AtMTP1 antibody. The protein band at 43 kDa was not detected when a corresponding antigen peptide was added to the reaction medium. Although background levels were apparently different between lanes 1, 3 and 4, the bands that appeared in lanes 1 and 3 did not appear in lanes 2 and 4 even when the background levels were much higher. A fusion protein of AtMTP1 with the V5 epitope and His_6 tag, which was expressed in yeast, was also detected by both anti-

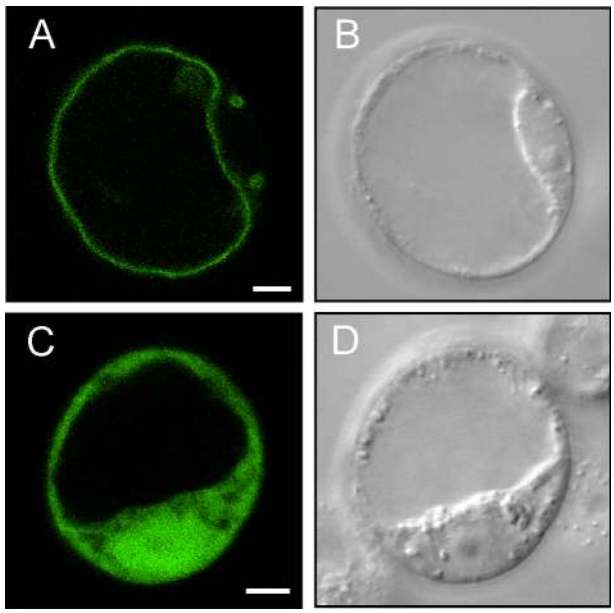

Fig. 3 Expression of AtMTP1–GFP fusion protein in protoplasts. The construct of *AtMTP1–GFP* was transiently expressed in *A. thaliana* suspension-cultured cells. Green fluorescence of AtMTP1–GFP was viewed by confocal laser scanning microscopy (A and C). The same protoplasts were viewed by differential interference contrast (DIC, B and D). Bar = 3 μm.

AtMTP1 (lane 3) and anti-His_6 antibodies (lane 5), but not in yeast with the control vector (lanes 4 and 6).

Subcellular localization of AtMTP1 in plant tissues

The crude membrane fraction prepared from the homogenate of root cells of *A. thaliana* cultured in a Murashige Skoog (MS) solution was subjected to equilibrium sucrose density gradient centrifugation (Fig. 2). AtMTP1 protein was recovered in fractions 9–13 together with the vacuolar H^+-ATPase subunit a (VHA-a). VHA-a is mainly localized to vacuolar membranes, although a part of VHA-a protein was detected in the endoplasmic reticulum (ER) and other endomembranes (Sze et al. 1999). Plasma membrane H^+-ATPase (AHA3) was recovered in fractions 18–21. Bip, an ER lumen marker protein, was also detected in the same fractions as AtMTP1 under the Mg^{2+}-free condition (Fig. 2A). In the presence of Mg^{2+} (Fig. 2B), peak fractions of Bip were moved to the high-density fractions 17–20, but the sedimentation of AtMTP1 was not altered. The activity of Triton-stimulated inosine diphosphatase (IDPase), a marker for the Golgi apparatus (Lord 1987), was detected in fractions 11–13, which partially overlapped that of AtMTP1. Thus, these results suggest that AtMTP1 is localized to the vacuolar membrane or Golgi apparatus in part, but not to plasma membrane or ER membrane. It should be noted that the 43 kDa band of AtMTP1 was clearly detected in the vacuolar membrane that was highly purified from *A. thaliana* suspension-cultured cells (Fig. 2C).

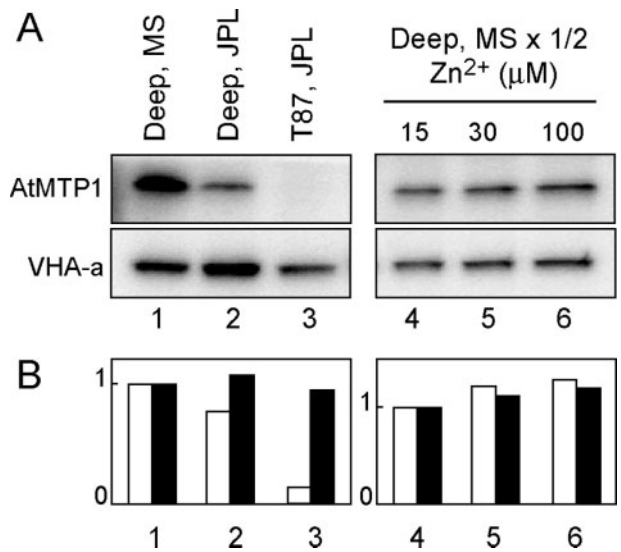

Fig. 4 Changes in AtMTP1 protein level under different concentrations of Zn. *A. thaliana* suspension-cultured cells, 'Deep' and T87 cells, were cultured for 4 d in the MS and JPL medium, which contained 30 and 11 μM Zn^{2+}, respectively (lanes 1–3). 'Deep' cells were cultured for 5 d in the one-half-strength MS medium that was supplemented with Zn to make a final concentration of 15, 30 or 100 μM, respectively (lanes 4–6). (A) Crude membranes were prepared from the cells and then an aliquot (20 μg) was subjected to immunoblotting with anti-AtMTP1 and anti-VHA-a antibodies. (B) The intensity of immunostained bands of AtMTP1 (white bars) and VHA-a (black bars) was determined densitometrically.

We also found a faint band with a smaller molecular size of 41 kDa in fractions 19–21. This band was different from the 43 kDa protein band detected in the vacuolar membrane fractions and the crude membranes prepared from *A. thaliana* 'Deep' cells (Fig. 2C). The 41 kDa band was not detected clearly in the crude membrane fractions from tissue homogenate and 'Deep' cells. Thus, a faint band of 41 kDa may be a non-specific band.

Detection of AtMTP1–GFP fusion protein on the vacuolar membrane

To determine the subcellular localization of AtMTP1, we prepared a DNA construct of a fusion protein of AtMTP1 with GFP (AtMTP1–GFP) and expressed it transiently in *A. thaliana* suspension-cultured cells. As shown in Fig. 3A, the green fluorescence from GFP was clearly detected on the vacuolar membrane, whereas fluorescence of free GFP was dispersed throughout the cytosol (Fig. 3C). It should be noted that GFP–AtMTP1, which contained GFP at the N-terminal end of AtMTP1, did not produce a clear fluorescent image. The N-terminal region of AtMTP1 may be critical for correct folding, and an additional GFP polypeptide might cause proteolytic degradation of the fusion protein.

Effects of cell types and the culture medium conditions on the AtMTP1 protein level

To examine whether the AtMTP1 protein level is altered by the Zn concentration in the medium, we immunochemically quantified AtMTP1 in suspension-cultured cells under various Zn concentrations. We used two types of *A. thaliana* suspension-cultured cells, 'Deep' and T87, which were cells developed from roots (Umeda et al. 1998) and whole seedlings (Axelos et al. 1992) of *A. thaliana* Columbia, respectively. When cells were cultured for 4 d in JPL medium, which contained 11 μM Zn, the AtMTP1 protein level was higher in 'Deep' cells rather than T87 cells (Fig. 4). Both cells seem to retain the memory of their original tissues. For example, T87 cells, but not 'Deep' cells, synthesize chlorophyll in the plastid and are green under the light. Micro array expression analysis (Wintz et al. 2003; Arabidopsis membrane protein library, http://www.cbs.umn.edu/arabidopsis/) and the Massively Parallel Signature Sequencing database (http://mpss.udel.edu/at/java.html) reported that the AtMTP1 mRNA level in roots is twice of that in shoots and leaves of *A. thaliana*. Therefore, the abundance of AtMTP1 in 'Deep' cells may be a reflection of its original tissue.

Although the content was extremely low, AtMTP1 was clearly detected in T87 cells. The AtMTP1 level varied with the medium. The AtMTP1 level in 'Deep' cells cultured in MS medium containing 30 μM Zn was three times greater than that of the cells in the JPL medium. Then we examined the effect of the Zn concentration in the culture medium on the AtMTP1 level. The level slightly increased with the concentration of Zn, but the change was similar to that of the V-ATPase subunit a (Fig. 4A and B, right panels). These results indicate that Zn in the medium even at 100 μM may not up-regulate the transcription or translation of AtMTP1 in suspension-cultured cells.

AtMTP1 knockout mutant showed enhanced susceptibility to Zn at high concentrations

We analyzed a T-DNA insertion mutant of *A. thaliana*. The insertion site of T-DNA was determined to be the 3′-terminal coding region of *AtMTP1* by DNA sequencing (Fig. 5A). The *mtp1-1* mutant lacked an *AtMTP1* transcription product, although the wild-type plant gave a band of 587 bp (Fig. 5B). AtMTP1 protein was not detected in the crude membrane fraction prepared from the mutant plant (data not shown).

The *mtp1-1* mutants were morphologically normal when grown in vitro and in the greenhouse under standard conditions. The wild-type and mutant plants were grown on MS medium for 2 weeks after germination, then transferred to the hydroponic medium containing 400 μM Zn for 2 d. Fig. 6 shows that the *mtp1-1* (–/–) homozygous mutant was highly sensitive to 400 μM Zn. However, the heterozygote *mtp1-1* (+/–) grew normally under the same conditions. The tolerance of the mutant plants to high concentrations of Zn was recovered when

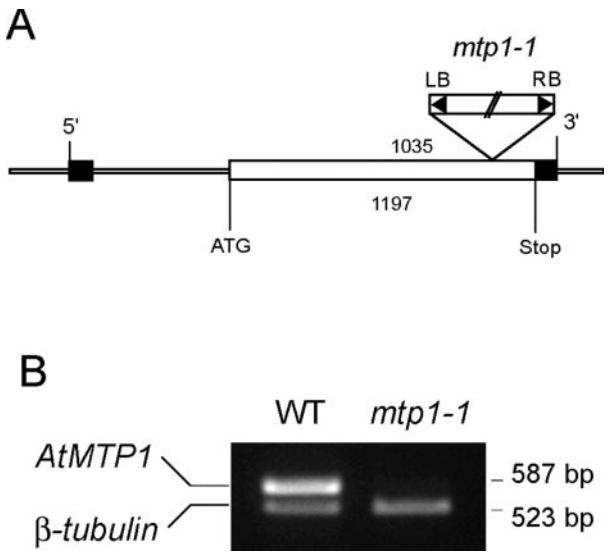

Fig. 5 (A) T-DNA integration site in *mtp1-1* mutant *A. thaliana*. The location of the T-DNA insertion within the sequence of the *AtMTP1* gene is shown. Filled boxes show the 5′- and 3′-UTRs and an open box shows the exon. The insertion site and the orientation of the T-DNA are indicated. (B) Detection of *AtMTP1* mRNA by RT–PCR. RT–PCR was performed on total RNA extracted from wild-type (WT) and *mtp1-1* mutant. Primers specific to β-tubulin were included as a control.

mtp1-1 was transformed with the *AtMTP1* gene under the control of the 35S promoter, confirming that *AtMTP1* is involved in the tolerance of *A. thaliana* to Zn.

The *mtp1-1* mutant plants grew normally in the MS medium like the wild-type plants. The MS medium contained 30 μM Zn. No difference in growth was observed between the *mtp1-1* mutant and wild-type seedlings when cultivated in the medium containing 30 or 80 μM Zn (Fig. 7A). The mutant plants did not grow in the presence of high concentrations of Zn (200 and 500 μM) (Fig. 7A). At 200 and 500 μM Zn, the root length of the mutant seedlings decreased to 60 and 10%, respectively, of that of the control seedlings grown in MS medium (30 μM Zn). Two-week-old plants germinated in MS medium were transferred to a cultivation solution containing 0, 1, 200 and 500 μM $ZnSO_4$ for 3 d (Fig. 7B). The *mtp1-1* mutant plantlets grew normally in 0 and 1 μM Zn; however, they showed severe chlorosis of leaves and suppression of leaf development in 200 and 500 μM Zn (Fig. 7B). It should be noted that the medium may contain a trace amount of Zn even in the 0 μM Zn culture medium, since no special measures were taken to remove completely metal ions contaminating either purified water or other reagents. Thus we could not draw any conclusions on the effect of complete Zn deficiency on the growth of the *mtp1-1* mutant.

AtMTP1 has been determined to transport Cd although at only 1% of the Zn transport rate (Bloß et al. 2002). We examined the sensitivity of *mtp1-1* mutants to other metals including Cd, by monitoring the root growth of germinating seedlings as shown in Fig. 7C. In the presence of 80 μM Co, 40 μM Cd or 40 μM Ni, the root length was 60–70% of that under control conditions (15 μM Zn). However, there was no difference between the wild type and the mutant plants. Manganese did not affect the growth even at 1.5 mM. These results suggest that AtMTP1 is highly specific to Zn at least at high concentrations of the metal. The negative effect of these metal ions at higher concentrations remains to be examined.

Changes in morphology of mtp1-1 mutant plants

In addition to the low growth rate of *mtp1-1* mutant seedlings in high concentrations of Zn, we observed a change in cell morphology. Figure 8 shows the sections prepared from mutant plants grown in 500 μM $ZnCl_2$. Plasmolysis tends to occur in cells of plants grown in the presence of high concentrations of Zn (Fig. 8B–E). As the major changes in the *mtp1-1* mutant plant, a large part of the parenchyma tissues in leaves was broken down and most mesophyll cells disappeared (Fig. 8C), while the breakdown of cells was not observed in the wild-type plant (Fig. 8B). The damage in leaves was more severe than that in roots, which did not have any collapsed cells (Fig. 8E). The collapse of cells may be a cause of etiolation of leaves in the mutant plants as observed in Fig. 6 and 7.

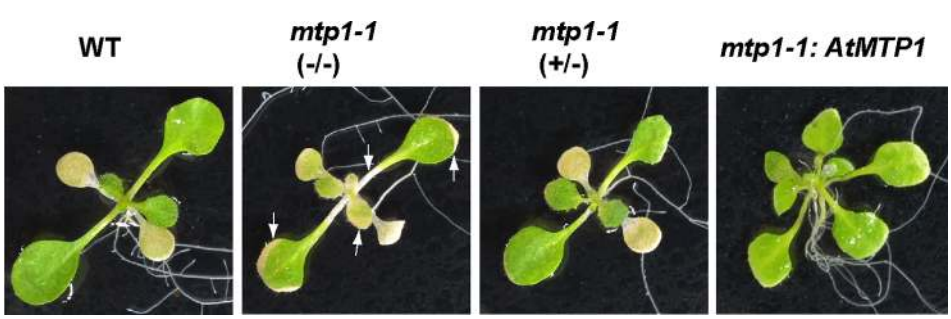

Fig. 6 Developmental defects in *mtp1-1* mutants at high Zn concentration. Wild-type and mutant plants were grown for 2 weeks (20 d for *mtp1-1:AtMTP1* plants) in the MS medium, which contained 30 μM $ZnSO_4$, and then for 48 h in the presence of 400 μM $ZnSO_4$. WT, wild-type plant; *mtp1-1* (–/–), *mtp1-1* homozygous mutant plant; *mtp1-1* (+/–), *mtp1-1* heterozygous mutant plant; *mtp1-1:AtMTP1*, transgenic *mtp1-1* mutant plant expressing *AtMTP1*. Arrows indicate severe chlorosis observed in homozygous mutant plants.

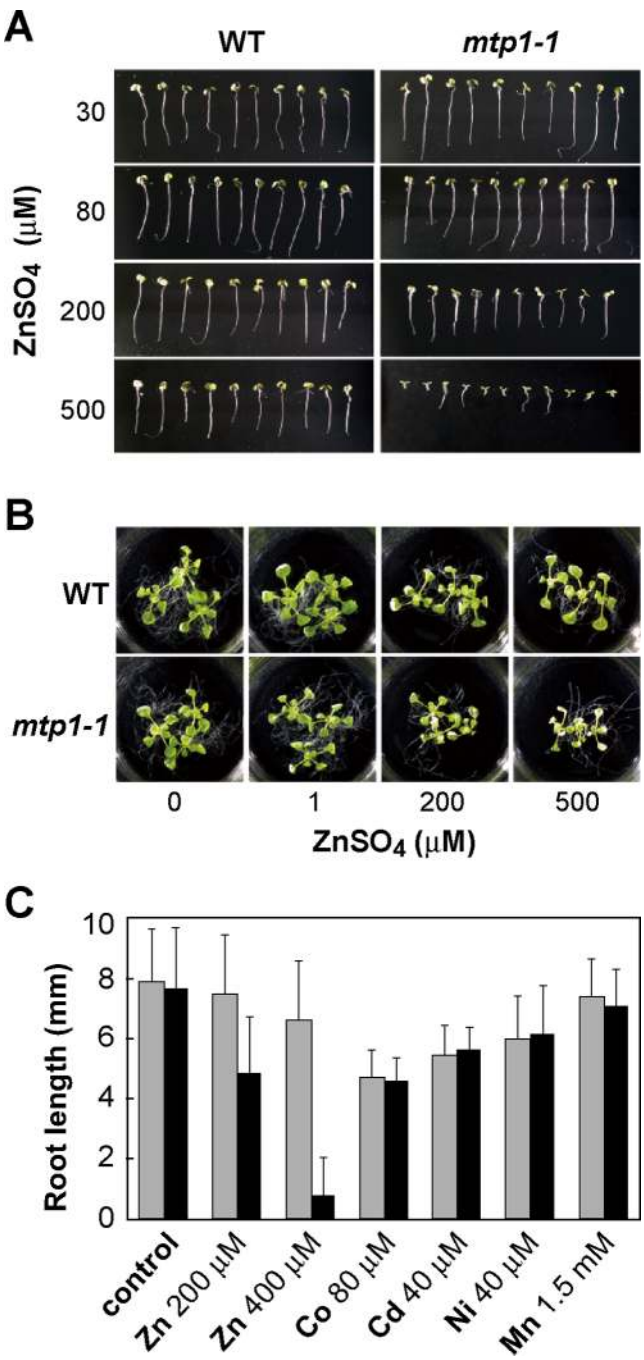

Fig. 7 Sensitivity of *mtp1-1* mutants to high Zn concentrations. (A) The wild-type (WT) and *mtp1-1* mutant plants were germinated for 4 d in the MS agar plates containing 30, 80, 200 and 500 μM of $ZnSO_4$ and then photographed. (B) The wild-type and *mtp1-1* mutant plants were grown for 2 weeks in the MS medium and then for 3 d in a solution supplemented with 0, 1, 200 or 500 μM $ZnSO_4$. (C) Root length of 4-day-old seedlings of *mtp1-1* plants grown in the MS plates supplemented with 200 μM $ZnSO_4$, 400 μM $ZnSO_4$, 80 μM $CoCl_2$, 40 μM $CdCl_2$, 40 μM $NiCl_2$ and 1.5 mM $MnCl_2$. The control seedlings were grown in one-half-strength MS medium (15 μM Zn).

Discussion

The extensive molecular and biochemical studies on AtMTP1, its homologs and orthologs have revealed that AtMTP1 translocates Zn (Bloß et al. 2002, Dräger et al. 2004, Kim et al. 2004). In this study, we determined the subcellular localization and physiological function of AtMTP1 *in planta*.

AtMTP1 is localized to vacuolar membranes of A. thaliana

Proteome analysis strongly suggested that AtMTP1 protein was localized at least to vacuolar membranes isolated from protoplasts of *A. thaliana* suspension-cultured cells (Shimaoka et al. 2004). However, other groups reported that plant MTP1 proteins were localized to other organelle membranes. A CDF family member, MTP1 from the Ni/Zn hyperaccumulator *Thlaspi goesingense*, has been shown to be localized to the plasma membranes of *A. thaliana* cells, which were transiently expressed with the GFP-tagged TgMTP1 (Kim et al. 2004). They estimated that the characteristics of metal-hyperaccumulating plants are achieved by increased xylem loading by the Zn efflux function of TgMTP1, and also suggested the dynamic relocalization of MTP1 between the plasma membranes and various endomembranes including vacuolar membranes as proposed for Zn homeostasis in mammalian systems (Huang et al. 2002). Delhaize et al. (2003) investigated a CDF member MTP1 (ShMTP1) of *Stylosanthes hamata*, a tropical legume able to grow normally in acid soils, and reported that the GFP-tagged ShMTP1 was localized to the vacuolar membranes of *A. thaliana* plants and tobacco cells and to the ER membranes of yeast. It was estimated that ShMTP1 acts to sequester Mn into the ER of yeast and into vacuoles in *A. thaliana*, although the Mn transport activity of ShMTP1 was not detected in the membrane vesicles derived from yeast and plants even under conditions of cation (Na^+, K^+ and H^+) gradients (Delhaize et al. 2003).

Mammalian Zn transporters (Znt1–Znt7) belonging to the CDF family have been characterized. Znt1 functions to enhance the efflux of Zn from the cytosol at the plasma membrane (Palmiter and Findley 1995). The other six Znt proteins are located in subcellular organelle membranes and are involved in sequestration of Zn into internal compartments (Huang et al. 2002, Kambe et al. 2002, Kirschke and Huang 2003). Furthermore, Znt4 and Znt6 have been reported to undergo Zn-induced membrane relocation from the *trans*-Golgi network to the plasma membrane (Huang et al. 2002).

The present study on the subcellular localization of AtMTP1 clearly showed that AtMTP1 is localized to the vacuolar membranes in suspension-cultured cells and tissues. First, subcellular fractionation of root tissues showed that most AtMTP1 protein was recovered in the vacuolar membrane (Fig. 2). The protein was also detected in the highly purified vacuolar membranes from suspension-cultured cells by immunoblotting. Magnesium shift experiments in the subcellular fractions indicated that AtMTP1 was not in the ER membrane. This is the first report of the vacuolar localization of AtMTP1

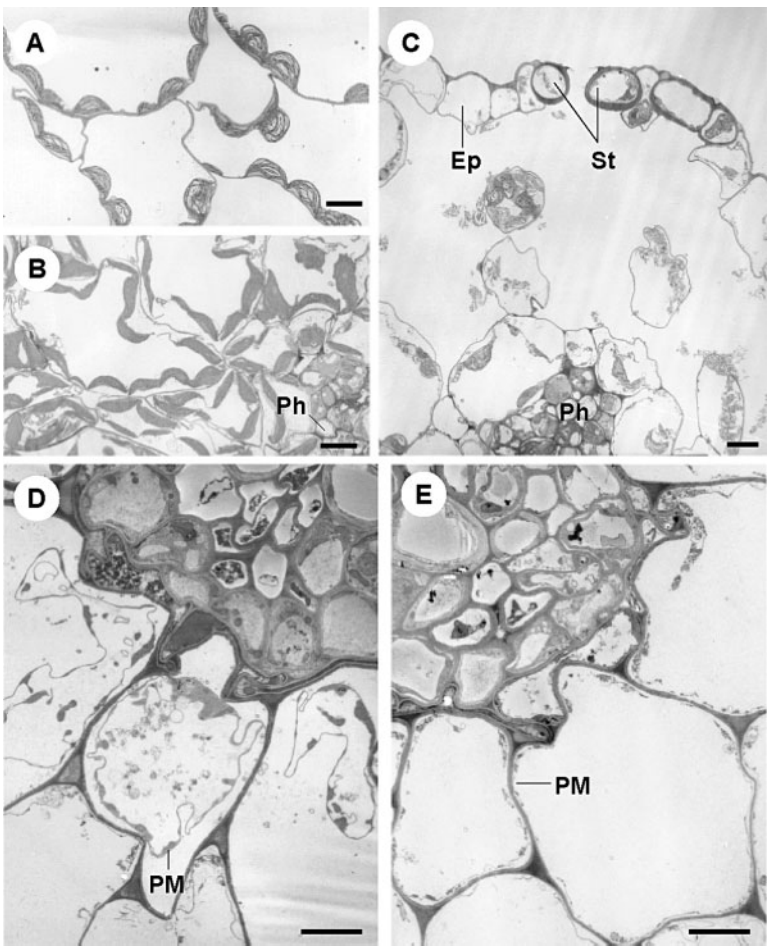

Fig. 8 Differences in morphology of cells in the wild-type and *mtp1-1* mutant plantlets. The wild-type (B and D) and *mtp1-1* mutant (C and E) seedlings were grown on MS plates for 2 weeks and then transferred to a solution containing 500 μM of $ZnSO_4$ for 24 h. Microsections from rosette leaves (B and C) and root (D and E) were observed by electron microscopy. (A) A section of mesophyll cells of rosette leaf grown for 2 weeks without $ZnSO_4$. Ep, epidermal cells; St, stomata cells; Ph, phloem cells; PM, plasma membrane. Bars = 5 μm.

protein without a tag. Secondly, the AtMTP1–GFP protein was clearly localized to the vacuolar membrane (Fig. 3). There is no signal on the Golgi apparatus and ER membranes in images of fluorescent microscopy of AtMTP1–GFP. In conclusion, AtMTP1 is localized predominantly to the vacuolar membranes, but not to the other organelle membranes, such as the ER, plasma and Golgi apparatus membranes.

In *T. goesingense* TgMTP1, the tagged protein was expressed in a different species *A. thaliana* (Kim et al. 2004). Probably, the plasma membrane localization may be due to the abnormal processes in the different species. For *S. hamata* ShMTP1, the GFP-tagged protein was detected in vacuolar membranes when expressed in tobacco cells and *A. thaliana*, but not in yeast (Delhaize et al. 2003). Along with the previous findings, the present study revealed that AtMTP1 functions to enhance Zn sequestration into vacuoles. Therefore, AtMTP1 may have a physiological role different from members of the ZRT, IRT-like protein (ZIP) family of *A. thaliana*, which are thought to be involved in the absorption of Zn from the soil (Guerinot 2000).

AtMTP1 is relatively constantly expressed

Several members of the ZIP family have been reported to be up-regulated markedly by Zn deficiency (Zhao and Eide 1996) and iron deficiency (Eide et al. 1996, Vert et al. 2001). In *A. halleri*, Zn hyperaccumulator markedly increased the transcriptional level of *MTP1* in root, but not in shoots, after 4 d of exposure to 100 and 300 μM Zn in the hydroponic solution (Dräger et al. 2004). We examined the changes in AtMTP1 in suspension-cultured cells, since suspension-cultured cells were thought to be more sensitive to external stresses than the cells in plantlets. However, the AtMTP1 content in the suspension-cultured cells was not affected markedly by the Zn concentration (Fig. 4). Our observation on the MTP1 protein apparently agrees with the previous study, which demonstrated that the mRNA levels of AtMTP1 were relatively constant at a wide range of Zn concentrations (van der Zaal et al. 1999). Thus, we speculate that AtMTP1 may function as a housekeeping enzyme in *A. thaliana*.

AtMTP1 is involved in the tolerance to high concentrations of Zn

There are two possible functions of AtMTP1 *in planta*. (i) Plant cells accumulate Zn in vacuoles through AtMTP1 to supply it in a Zn-deficient condition. Zn is an essential component of >300 plant enzymes including RNA polymerase, Cu/Zn superoxide dismutase and carbonic anhydrase. A large number of proteins contain Zn-binding structural domains such as the zinc finger domain. AtMTP1 may act to transport Zn to the vacuolar Zn pool when available Zn exists in the cytosol. (ii) The cells exclude excess Zn in the cytosol into vacuoles through AtMTP1 to avoid the toxicity. Although Zn is an essential micronutrient, the metal can be toxic at supraoptimal concentrations like other micronutrients. Uncontrolled binding can render enzymes non-functional and the redox activity can elicit the generation of reactive oxygen species (Weber et al. 2004). The negative effect was observed in the present study. At concentrations exceeding 200 μM, Zn markedly inhibited the growth of the whole plants and roots (Fig. 6, 7A).

The present results suggest the latter function (ii). The *mtp1-1* plants suffered severe damage when grown in the presence of high Zn concentrations (Fig. 7), but showed no damage when grown without Zn for 3 d (Fig. 7B). In the presence of Zn at concentrations exceeding 200 μM, the *mtp1-1* plants, which are mutants lacking AtMTP1, cannot grow normally. This severe damage could be recovered by introducing *AtMTP1* into the mutant (Fig. 6). Our observation is in agreement with the previous demonstration that transgenic plants with *ZAT1* (*AtMTP1*) under control of the cauliflower mosaic virus 35S promoter exhibited enhanced resistance to Zn at 250 μM (van der Zaal et al. 1999). The physiological function seems to be similar to that of a poplar MTP1, which was also located in the vacuolar membrane and conferred Zn tolerance (Blaudez et al. 2003).

Severe phenotypic changes were not observed in the *mtp1-1* plants under low Zn concentrations (Fig. 7B), but we cannot deny the possibility that MTP1 plays the function (i) described above and other isoforms may complement the *mtp1-1* mutation. In this study, plantlets were grown in Zn-containing medium and then transferred to the medium without Zn. The mutant plantlets were able to grow normally even under the Zn-deficient condition by using Zn accumulated in the vacuoles. Further study using a Zn-specific chelator may provide clear information of the effect of the complete Zn deficiency on the physiological properties of the *mtp1-1* mutant.

We speculate that AtMTP1 may act to exclude excess Zn from the cytosol into vacuoles, which occupy a large part of the cell. The efflux through the plasma membrane may also be involved in the tolerance to Zn. The Zn content in the apoplastic space may increase when plants are grown in the presence of supraoptimal Zn concentrations, under which exclusion of Zn into the cell wall space may be impossible. Thus, the function (ii) of AtMTP1 may be essential under these conditions.

Damage in tissues of mtp1-1 mutant plants

Zn is a micronutrient, and symptoms caused by its deficiency are well known in plants (Marschner 1995). The above results demonstrated that Zn at high concentrations is harmful to the *mtp1-1* mutant of *A. thaliana*. Even when the mutant was exposed to 500 μM Zn for only 24 h, the leaf and root tissues, especially leaf mesophyll cells, became degraded (Fig. 8). Under these conditions, apoptosis may have occurred in the tissues of the AtMTP1-lacking mutant, although further experimental evidence should be obtained. These symptoms were observed only in the mutant plantlets, not in the wild-type plants. The present results clearly indicate two points: (i) Zn is toxic to *A. thaliana* at excess concentrations; and (ii) AtMTP1 is essential for protection of plant tissues from high concentrations of Zn. To confirm the toxicity of Zn, we will need to perform further molecular genetic and cell biological analyses.

In conclusion, the results of the present study offer insight into a molecular pathway of Zn sequestration in non-hyperaccumulator plants. Although an additional Zn detoxification mechanism, for instance metal exclusion out of the cell and/or chelating of Zn, may exist in *A. thaliana*, we provide clear evidence that AtMTP1 is a key element of the indispensable Zn sequestration system in *A. thaliana*. For further understanding of the Zn homeostasis in plant cells, the Zn concentration and the mechanism of the tissue breakdown in *mtp1-1* mutant plants should be investigated.

Materials and Methods

Plant materials and growth conditions

Surface-sterilized seeds of *A. thaliana* (ecotypes, Col-0 and WS) were germinated on sterile MS-salt plates containing 2.3 mM MES-KOH, pH 5.7, 1% sucrose for growing the roots with shaking in a rotary shaker (100 rpm). All plants were grown at 23°C under long-day conditions (light/dark regime of 16 h/8 h, cool-white lamp). *A. thaliana* (ecotype, Columbia) suspension-cultured cells ('Deep' cells; previous name, Col-0 cells), which originated from roots, were a kind gift from Dr. Masaaki Umeda of Tokyo University, and were cultured as described previously (Umeda et al. 1998). T87 cells, which were prepared from whole seedlings of *A. thaliana* (Axelos et al. 1992, Nakamichi et al. 2004), were also used. In some experiments, cells were cultured in JPL medium containing 19 mM KNO_3, 1 mM $CaCl_2$, 0.45 mM $MgSO_4$, 0.4 mM KH_2PO_4, 0.15 mM Na_2HPO_4, 30 μM H_3BO_3, 30 μM $MnSO_4$, 11 μM $ZnSO_4$, 1.6 μM KI, 0.3 μM Na_2MoO_4, 32 nM $CoCl_2$, 3 nM $CuSO_4$, 20 μM $FeSO_4$ and 20 μM Na_2-EDTA. The MS medium contained 19 mM KNO_3, 3 mM $CaCl_2$, 1.5 mM $MgSO_4$, 1.2 mM KH_2PO_4, 0.1 mM H_3BO_3, 0.1 mM $MnSO_4$, 30 μM $ZnSO_4$, 5.2 μM KI, 1.0 μM Na_2MoO_4, 0.1 μM $CoCl_2$, 0.1 μM $CuSO_4$, 0.1 mM $FeSO_4$, 0.1 mM Na_2-EDTA, and 21 mM NH_4NO_3 as minerals. In experiments described in Fig. 6 and 7B, we used a cultivation solution, which contained 0.28 mM KH_2PO_4, 1.25 mM KNO_3, 1.5 mM $Ca(NO_3)_2$, 0.75 mM $MgSO_4$, 5 μM Fe(III)-EDTA, 25 μM H_3BO_3, 5 μM $MnCl_2$, 0.5 μM $CuSO_4$, 50 μM KCl and 0.1 μM Na_2MoO_4, buffered at pH 5.7 with 3 mM MES-KOH (pH 5.7).

Subcellular fractionation of Arabidopsis tissues and cells

Roots of 30-day-old plants, in hydroponic culture, were homogenized in a homogenizing medium containing 50 mM Tris–HCl, pH 8.0,

250 mM sorbitol, 10 mM EDTA, 4 mM dithiothreitol, 0.1% 2-mercaptoethanol and 100 μM *p*-(amidinophenyl) methanesulfonyl fluoride hydrochloride (APMSF). The homogenate was filtered through four layers of Miracloth (EMD Biosciences, Darmstadt, Germany), and centrifuged at 10,000×*g* for 10 min. The supernatant was centrifuged at 100,000×*g* for 30 min and then the precipitate was suspended in homogenizing medium. The suspension (crude membranes) was layered on sucrose density gradients (11 ml, 15–45%), centrifuged at 77,000×*g* for 17 h, and then fractionated into 0.5 ml fractions.

Intact vacuoles were prepared from the protoplasts of *A. thaliana* suspension-cultured cells and then the highly purified preparation of vacuolar membranes was prepared from the isolated vacuoles as described previously (Shimaoka et al. 2004).

Preparation of antibodies

For preparation of antibodies, a peptide corresponding to the N-terminal region of AtMTP1 (At2g46800, positions 37–50, CGFSDSKNASGDAHE) was synthesized, linked with keyhole limpet hemocyanin, and then injected into rabbits. The peptide-specific antibodies against the plasma membrane H^+-ATPase (AHA3, At5g57350, positions 690–704, CTISKDRVKPSPTPDS; an additional cysteine is underlined), Bip (At5g42020, positions 285–298, SKDNKALGKLRREC) and subunit a of vacuolar H^+-ATPase (AtVHA-a, At2g21410, positions 117–135, ELVEINANNDKLQRSYNELC) were also prepared by the same procedure.

SDS–PAGE and immunoblotting

Proteins were separated by SDS–PAGE, and transferred to an Immobilon-P membrane (Millipore, Billerica, USA). After blocking with de-fatted milk, the membrane filter was incubated with primary antibody (2,000-fold dilution) and then with horseradish peroxidase-conjugated protein A. In control experiments, the corresponding antigen peptide was added to the first antibody solution before incubation with the blot membrane at a concentration of 1.5 μg ml^{-1}. The mixture was incubated for 30 min at 22°C and then used for immunoblotting. Chemiluminescent reagents ECL (Amersham Biosciences, Buckinghamshire, UK) and Super Signal (Pierce Biotechnology, Rockford, CA) were used for detection of antigens.

PCR cloning of AtMTP1 and expression in yeast

For isolation of the *AtMTP1* cDNA, total RNA was isolated from 3-week-old *Arabidopsis* seedlings, and converted to cDNAs using Superscript™ II RNase H– reverse transcriptase (Invitrogen, Carisbad, USA) and an oligo(dT) adapter primer [5′-CGGGATCCACTAGTTCTAGAGCGC$(T)_{17}$-3′]. *AtMTP1* cDNAs were then directly amplified by polymerase chain reaction (PCR) with a pair of primers: 5′-CACCATGGAGTCTTCAAGTCC-3′ (forward) and 5′-GCGCTCGATTTGTATCGTG-3′ (reverse). The cDNA was inserted into a Gateway entry vector pENTR/D-TOPO (Invitrogen), and then the *AtMTP1* DNA was introduced into yeast expression vector pYES/DEST52 (Invitrogen) by the Gateway system (Invitrogen). The plasmid was transferred into yeast strain W303 (*MAT***a** *leu2 ura3 his3 trp1 ade2 can1-100*) by the LiOAc/PEG method (Gietz et al. 1995) and grown in SC minimal medium (Invitrogen). AtMTP1 was expressed under the control of the *GAL1* promoter in SC minimal galactose medium. Crude membranes were prepared from yeast cells cultured for 24 h at 30°C as described previously (Nakanishi et al. 2001). The AtMTP1 was detected by immunoblotting.

Transient transformation of Arabidopsis suspension-cultured cells

Fusion proteins with GFP were produced by inserting the PCR products of AtMTP1 into a newly prepared Gateway vector New-pUGW5 (developed by Tsuyoshi Nakagawa) using the Gateway system (Invitrogen). It was transiently expressed in *A. thaliana* suspension-cultured cells as described previously (Ueda et al. 2001, Uemura et al. 2004) with a few modifications. Cultured cells were incubated in enzyme solution for 80 min at 30°C under gentle agitation to prepare protoplasts and then passed through a nylon mesh (41 μm pore). Protoplasts containing the plasmid were incubated with gentle agitation at 23°C for 12 h in the dark. Transformed cells were viewed using a confocal laser microscope (FV500, Olympus, Tokyo, Japan) and recorded by a charge-coupled device (CCD) camera (DP50, Olympus).

Characterization of the AtMTP1 T-DNA insertion line

The T-DNA insertion line in *AtMTP1* (FLAG-539A04) was obtained from the source of *Arabidopsis* T-DNA insertion lines made by Laboratoire de Génétique et Amélioration des Plantes, Institut National de la Recherche Agronomique, Versailles. A homozygous transgenic line was selected and the location of the T-DNA insertion in *AtMTP1* was determined by PCR with an *AtMTP1*-specific (5′-GGGTGACTGTTACCACTCATCACCATC-3′) and T-DNA-specific Tag5 in the left border (5′-CTACAAATTGCCTTTTCTTATCGAC-3′) primers. For the mutant complementation, the MTP1 gene on the pENTR-MTP1 entry vector was cloned in pGWB2 binary vector with the 35S promoter of cauliflower mosaic virus, and introduced into *Agrobacterium tumefaciens* GV3101::PM90 strain and then used to transform *mtp1-1* homozygous mutant plants by the floral dip method (Clough and Bent 1988).

Electron microscopy

For transmission electron microscopy, 2-week-old rosette leaves or roots were cut into 1 mm wide pieces. Tissue was fixed overnight at 4°C in 4% paraformaldehyde and 2% glutaraldehyde in 0.1 M cacodylic acid buffer, pH 7.4, and then washed four times for 15 min each in 0.1 M cacodylic acid buffer, pH 7.4, and post-fixed in 1% OsO_4 for 4 h. After three washes of 5 min each in 0.1 M cacodylic acid buffer, pH 7.4, tissue was dehydrated through an ethanol series (50–100%) for 20 min each at room temperature. The tissue was infiltrated with an epoxy resin (EPON812; TAAB Laboratories, Berkshire, UK) at 60°C for 2 d. Ultrathin sections were viewed counter-stained with uranyl acetate and lead citrate and examined with a JEOL (Tokyo, Japan) JEM2000 EX transmission electron microscope.

Acknowledgment

We are grateful to Fumiyoshi Ishikawa for his assistance in the transient expression in protoplast, to Yoko Hotta for assisting in the immunoblot analysis, and to Dr. Masaaki Umeda (the University of Tokyo, Japan) for providing *A. thaliana* suspension 'Deep' cells. We thank INRA Versailles for providing seeds of the *AtMTP1* insertion line. This work was supported by Grants-in-Aid for Scientific Research 16380068, 13CE2005 and 14COEA2 from the Ministry of Education, Sports, Culture, Science and Technology of Japan.

References

Axelos, M., Curie, C., Mazzolini, L., Bardet, C. and Lescure, B. (1992) A protocol for transient gene expression in *Arabidopsis thaliana* protoplasts isolated from cell suspension cultures. *Plant Physiol. Biochem.* 30: 123–128.

Becker, M., Talke, I.N., Krall, L. and Krämer, U. (2004) Crossspecies microarray transcript profiling reveals high constitutive expression of metal homeostasis genes in shoots of the zinc hyperaccumulator *Arabidopsis halleri*. *Plant J.* 37: 251–268.

Blaudez, D., Kohler, A., Martin, F., Sanders, D. and Chalot, M. (2003) Poplar metal tolerance protein 1 confers zinc tolerance and is an oligomeric vacu-

olar zinc transporter with an essential leucine zipper motif. *Plant Cell* 15: 2911–2928.

Bloß, T., Clemens, S. and Nies, D.H. (2002) Characterization of the ZAT1p zinc transporter from *Arabidopsis thaliana* in microbial model organisms and reconstituted proteoliposomes. *Planta* 214: 783–791.

Clemens, S., Palmgren, M.G. and Krämer, U. (2002). A long way ahead: understanding and engineering plant metal accumulation. *Trends Plant Sci.* 7: 309–315.

Clough, S.J. and Bent, A.F. (1988) Floral dip: a simplified method for *Agrobacterium*-mediated transformation of *Arabidopsis thaliana*. *Plant J.* 16: 735–743.

Delhaize, E., Kataoka, T., Hebb, D.M., White, R.G. and Ryan, P.R. (2003) Genes encoding proteins of the cation diffusion facilitator family that confer manganese tolerance. *Plant Cell* 15: 1131–1142.

Dräger, D.B., Desbrosses-Fonrouge, A.G., Krach, C., Chardonnens, A.N., Meyer, R.C., Saumitou-Laprade, P. and Krämer, U. (2004) Two genes encoding *Arabidopsis halleri* MTP1 metal transport proteins co-segregate with zinc tolerance and account for high MTP1 transcript levels. *Plant J.* 39: 425–39.

Eide, D., Broderius, M., Fett, J. and Guerinot, M.L. (1996) A noveliron-regulated metal transporter from plants identified by functional expression in yeast. *Proc. Natl Acad. Sci. USA* 93: 5624–5628.

Gietz, R.D., Schiestl, R.H., Willems, A.R. and Woods, R.A. (1995) Studies on the transformation of intact yeast cells by the LiAc/SS-DNA/PEG procedure. *Yeast* 11: 355–360.

Guerinot, M.L. (2000) The ZIP family of metal transporters. *Biochim. Biophys. Acta* 1465: 190–198.

Huang, L., Kirschke, C.P. and Gitschier, J. (2002) Functional characterization of a novel mammalian zinc transporter, ZnT6. *J. Biol. Chem.* 277: 26389–26395.

Kambe, T., Narita, H., Yamaguchi-Iwa, Y., Hirose, J., Amano, T., Sugiura, N., Sasaki, R., Mori, K., Iwanaga, T. and Nagao, M. (2002) Cloning and characterization of a novel mammalian zinc transporter, zinc transporter 5, abundantly expressed in pancreatic β-cells. *J. Biol. Chem.* 277: 19049–19055.

Kim, D., Gustin, J.L., Lahner, B., Persans, M.W., Baek, D., Yun, D.J. and Salt, D.E. (2004) The plant CDF family member TgMTP1 from the Ni/Zn hyperaccumulator *Thlaspi goesingense* acts to enhance efflux of Zn at the plasma membrane when expressed in *Saccharomyces cerevisiae*. *Plant J.* 39: 237–251.

Kirschke, C.P. and Huang, L. (2003) ZnT7, a novel mammalian zinc transporter, accumulates zinc in the Golgi apparatus. *J. Biol. Chem.* 278: 4096–4102.

Küpper, H., Zhao, F.J. and McGrath, S.P. (1999) Cellular compartmentation of zinc in leaves of the hyperaccumulator *Thlaspi caerulescens*. *Plant Physiol.* 119: 305–311.

Küpper, H., Lombi, E., Zhao, F.J. and McGrath, S.P. (2000) Cellular compartmentation of cadmium and zinc in relation to other elements in the hyperaccumulator *Arabidopsis halleri*. *Planta* 212: 75–84.

Lord, M.J. (1987) Isolation of endoplasmic reticulum: general principles, enzymatic markers, and endoplasmic reticulum-bound polysomes. *Methods Enzymol.* 148: 576–584.

Marschner, H. (1995) Function of mineral nutrients: micronutrients. *In* Mineral Nutrition of Higher Plants, 2nd edn. Edited by Marschner, H. pp. 347–364. Academic Press, London.

Nakamichi, N., Ito, S., Oyama, T., Yamashino, T., Kondo, T. and Mizuno, T. (2004) Characterization of plant circadian rhythms by employing *Arabidopsis* cultured cells with bioluminescence reporters. *Plant Cell Physiol.* 45: 57–67.

Nakanishi, Y., Saijo, T., Wada, Y. and Maeshima, M. (2001) Mutagenic analysis of functional residues in putative substrate-binding site and acidic domains of vacuolar H^+-pyrophosphatase. *J. Biol. Chem.* 276: 7654–7660.

Palmiter, R.D. and Findley, S.D. (1995) Cloning and functional characterization of a mammalian zinc transporter that confers resistance to zinc. *EMBO J.* 14: 639–649.

Persans, M.W., Nieman, K. and Salt, D.E. (2001) Functional activity and role of cation-efflux family members in Ni hyperaccumulation in *Thlaspi goesingense*. *Proc. Natl Acad. Sci. USA* 98: 9995–10000.

Sarret, G., Saumitou-Laprade, P., Bert, V., Proux, O., Hazemann, J.L., Traverse, A., Marcus, M.A. and Manceau, A. (2002) Forms of zinc accumulated in the hyperaccumulator *Arabidopsis halleri*. *Plant Physiol.* 130: 1815–1826.

Shimaoka, T., Ohnishi, M., Sazuka, T., Mitsuhashi, N., Hara-Nishimura, I., Shimazaki, K., Maeshima, M., Yokota, A., Tomizawa, K. and Mimura, T. (2004) Isolation of intact vacuoles and proteomic analysis of tonoplast from suspension-cultured cells of *Arabidopsis thaliana*. *Plant Cell Physiol.* 45: 672–683.

Sze, H., Li, X. and Palmgren, M.G. (1999) Energization of plant cell membranes by H^+-pumping ATPases: regulation and biosynthesis. *Plant Cell* 11: 677–689.

Thompson, J.D., Higgins, D.G. and Gibson, T.J. (1994) CLUSTAL W: improving the sensitivity of progressive multiple sequence alignment through sequence weighting, position-specific gap penalties and weight matrix choice. *Nucleic Acids Res.* 22: 4673–4780.

Ueda, T., Yamaguchi, M., Uchimiya, H. and Nakano, A. (2001) Ara6, a plant unique novel type Rab GTPase, functions in the endocytic pathway of *Arabidopsis thaliana*. *EMBO J.* 20: 4730–4741.

Uemura, T., Ueda, T., Ohniwa, R.L., Nakano, A., Takeyasu, K. and Sato, M.H. (2004) Systematic analysis of SNARE molecules in *Arabidopsis*: dissection of post-Golgi network pathways in plants. *Cell Struct. Funct.* 29: 49–65.

Umeda, M., Bhalerao, R.P., Schell, J., Uchimiya, H. and Koncz, C. (1998) A distinct cyclin-dependent kinase-activating kinase of *Arabidopsis thaliana*. *Proc. Natl Acad. Sci. USA* 95: 5021–5026.

van der Zaal, B.J., Neuteboom, L.W., Pinas, J.E., Chardonnens, A.N., Schat, H., Verkleij, J.A.C. and Hooykaas, P.J.J. (1999) Overexpression of a novel *Arabidopsis* gene related to putative zinc-transporter genes from animals can lead to enhanced zinc resistance and accumulation. *Plant Physiol.* 119: 1047–1056.

Vert, G., Briat, J.F. and Curie, C. (2001). Arabidopsis IRT2 gene encodes a root–periphery iron transporter. *Plant J.* 26: 181–189.

Weber, M., Harada, E., Vess, C., Roepenack-Lahaye, E. and Clemens, S. (2004) Comparative microarray analysis of *Arabidopsis thaliana* and *Arabidopsis halleri* roots identifies nicotianamine synthase, a ZIP transporter and other genes as potential metal hyperaccumulation factors. *Plant J.* 37: 269–281.

Wintz, H., Fox, T., Wu, Y.Y., Feng, V., Chen, W., Chang, H.S., Zhu, T. and Vulpe, C. (2003) Expression profiles of *Arabidopsis thaliana* in mineral deficiencies reveal novel transporters involved in metal homeostasis. *J. Biol. Chem.* 278: 47644–47653.

Zhao, H. and Eide, D. (1996) The *ZRT2* gene encodes the low affinity zinc transporter in *Saccharomyces cerevisiae*. *J. Biol. Chem.* 271: 23203–23210.

Zhao, F.J., Lombi, E., Breedon, T. and Mcgrath, S.P. (2000) Zinc hyperaccumulation and cellular distribution in *Arabidopsis halleri*. *Plant Cell Environ.* 23: 507–514.

(Received October 22, 2004; Accepted November 4, 2004)